



# Template-free synthesis, characterization and photoluminescence of hierarchical persimmon-shaped $\text{CeF}_3:\text{Tb}^{3+}$ microstructures



Yanfeng Tang, Jinli Zhu, Tongming Sun, Xinlin Shen, Guoqing Jiang\*

School of Chemistry and Chemical Engineering, Nantong University, Nantong 226019, PR China

## ARTICLE INFO

### Article history:

Received 7 April 2013

Accepted 25 May 2013

Available online 31 May 2013

### Keywords:

$\text{CeF}_3$   
Hierarchical  
Crystal growth  
Microstructure  
Luminescence

## ABSTRACT

Employing  $\text{N}(\text{C}_4\text{H}_9)_4\text{BF}_4$  as fluoride source, large scale multilayer-stacked hierarchical persimmon-shaped  $\text{CeF}_3$  architectures have been prepared via a facile and template-free hydrothermal route. The crystalline phase and morphology of the as-prepared hierarchical  $\text{CeF}_3$  microcrystals were investigated by X-ray powder diffraction (XRD) and scanning electron microscopy (SEM). The results revealed that uniform and monodispersed hierarchical nanodisk-assembled persimmon-shaped  $\text{CeF}_3$  microcrystals with average diameters of  $3\ \mu\text{m}$  can be easily synthesized. The effects of synthesis parameters, as well as fluoride source and reaction time were systematically investigated. The room temperature photoluminescence (PL) properties of these different morphological  $\text{CeF}_3:\text{Tb}^{3+}$  were measured.

© 2013 Elsevier B.V. All rights reserved.

## 1. Introduction

In recent years, 3D hierarchical architectures built from nanoscale units in a particular way, have attracted considerable attention not only due to the fundamental scientific interest but also for potential technological applications [1–3]. Many efforts have been dedicated to develop new methods for the fabrication of high-quality hierarchical nano/microstructures in different systems. As we all know, chelating agents or surfactants always play an important role in controlling the crystal growth and determining the final morphology of the hierarchical nano/microstructures. However, the addition of chelating agents or surfactants usually involves a complicated process and may result in impurities in products. Therefore, the development of facile, template-free and one-step method for the fabrication of uniform hierarchical architectures are of great scientific and technical interests.

Within the last several years, cerium fluoride ( $\text{CeF}_3$ ) has attracted increasing attention as an inorganic scintillating crystal and important fluorescent host material [4–5], because of its high density, fast response, high-energy physics, high-radiation resistance, low vibrational energies and the subsequent minimization of the quenching of the excited state of the rare-earth ions. Meanwhile, studies also indicate that  $\text{CeF}_3$  is a good solid lubricant as a result of its layered structure [6]. Many chemical synthesis techniques have been developed to fabricate the  $\text{CeF}_3$  and  $\text{Ln}^{3+}$ -doped  $\text{CeF}_3$  materials, such as hydrothermal methods [7–10], polyol method [5,11], ultrasonic routes [12–14], microwave

irradiation route [15,16], reverse micelles or microemulsions [6,17,18]. Correspondingly,  $\text{CeF}_3$  and  $\text{Ln}^{3+}$ -doped  $\text{CeF}_3$  with multi-form structures and morphologies have been prepared, such as nanoparticles, spheres, triangular nanoplates, hexagon-shaped nanoplates, nanodisks, nanorods and nanowires. However, little report has been devoted to the preparation of well-dispersed  $\text{CeF}_3$  hierarchical architectures. Herein, by using  $\text{N}(\text{C}_4\text{H}_9)_4\text{BF}_4$  as the fluoride source, unique multilayer-stacked hierarchical persimmon-shaped  $\text{CeF}_3$  architectures were prepared via a facile hydrothermal route. Moreover, the room-temperature PL properties of  $\text{Tb}^{3+}$  doped  $\text{CeF}_3$  were investigated. It is proposed that fluoride source and reaction time all played crucial roles in the formation of hierarchical persimmon-shaped  $\text{CeF}_3$ .

## 2. Experimental section

All the chemicals used in this work such as  $\text{Ln}(\text{NO}_3)_3 \cdot 6\text{H}_2\text{O}$  ( $\text{Ln} = \text{Ce}, \text{Tb}$ ),  $\text{N}(\text{C}_4\text{H}_9)_4\text{BF}_4$ ,  $\text{N}(\text{CH}_3)_4\text{BF}_4$  and  $\text{NH}_4\text{BF}_4$  were analytical grade and without any further purification. A typical procedure for the preparation of  $\text{CeF}_3$  is given below. 1.0 mmol  $\text{Ce}(\text{NO}_3)_3 \cdot 6\text{H}_2\text{O}$  was added to 25 mL distilled water under stirring, when these reagents were dissolved, 1.0 mmol  $\text{N}(\text{C}_4\text{H}_9)_4\text{BF}_4$  was added to the solution. After stirring for 20 min, the obtained suspension was transferred into a 30 mL Teflon lined autoclave. The autoclave was sealed and heated at  $120\ ^\circ\text{C}$  for 12 h, then cooled to room temperature naturally. The solid products were precipitated by centrifugation, washed with distilled water and ethanol and finally dried under vacuum at  $70\ ^\circ\text{C}$  for 3 h.  $\text{Tb}^{3+}$  doped  $\text{CeF}_3$  samples were prepared by the same procedure except for an additional 5%

\* Corresponding author. Tel./fax: +86 513 85012872.  
E-mail address: [jgq@ntu.edu.cn](mailto:jgq@ntu.edu.cn) (G. Jiang).

(total molar ratio)  $\text{Tb}(\text{NO}_3)_3 \cdot 6\text{H}_2\text{O}$  added into the  $\text{Ce}(\text{NO}_3)_3 \cdot 6\text{H}_2\text{O}$  solution at the initial stage.

The crystalline phases of the products were analyzed by Bruker AXSD8 ADVANCE X-ray diffractometer (Cu  $K\alpha$  radiation  $\lambda=0.15418$  nm). The sizes and morphologies of the products were characterized by SEM on Hitachi S-4800. The luminescence

spectra of the samples were recorded on HITACHI F-4500 spectrophotometer at room temperature.

### 3. Results and discussion

The crystal structure and phase purity of the samples were characterized by XRD. Fig. 1 shows the XRD of the as-synthesized  $\text{CeF}_3$  samples. The X-ray diffraction pattern of the product prepared with a molar ratio of  $\text{N}(\text{C}_4\text{H}_9)_4\text{BF}_4/\text{Ce}^{3+}$  of 0.75:1 within 12 h is shown in Fig. 1a. All of the diffraction peaks can be indexed to the hexagonal phase of  $\text{CeF}_3$  by comparison with the data from JCPDS card no. 08-0045. No peaks of any other phases or impurities were detected. When other reaction conditions were kept identical, the XRD patterns of the products obtained from 3 h and 6 h are shown in parts b and c of Fig. 1, respectively. The diffraction peaks of the samples obtained from 1 h (or 12 h) are sharper than those of the product obtained after reaction for 3 h, suggesting the improved crystallinity of the product after prolonging the reaction time. On the other hand, when the fluoride source are changed to  $\text{N}(\text{CH}_3)_4\text{BF}_4$  and  $\text{NH}_4\text{BF}_4$ , the XRD results are shown in Fig. 1d and e. The results indicated that changing of the reaction parameters (fluoride source, reaction time) have no obvious effects on the crystalline phase of the products.

The sizes and morphologies of the as-prepared  $\text{CeF}_3$  products were characterized by SEM. Fig. 2a–d showed the typical SEM images of the as-prepared  $\text{CeF}_3$  from different reaction periods when the molar ratio of  $\text{N}(\text{C}_4\text{H}_9)_4\text{BF}_4/\text{Ce}^{3+}$  was fixed as 0.75:1.

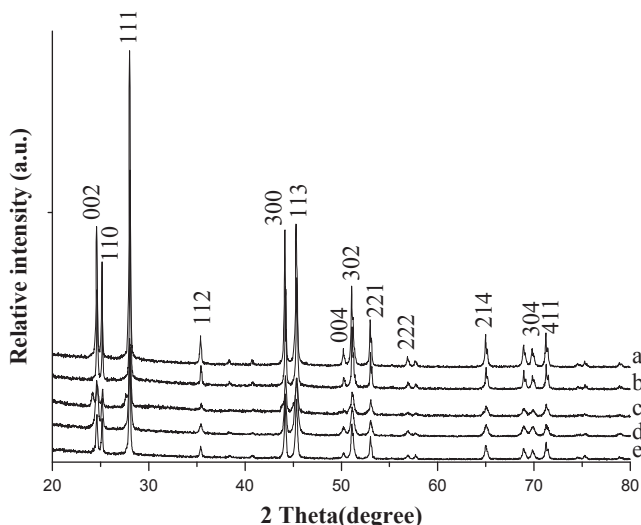


Fig. 1. XRD pattern of the  $\text{CeF}_3$  prepared from (a–c)  $\text{N}(\text{C}_4\text{H}_9)_4\text{BF}_4$ , (d)  $\text{N}(\text{CH}_3)_4\text{BF}_4$  and (e)  $\text{NH}_4\text{BF}_4$ .

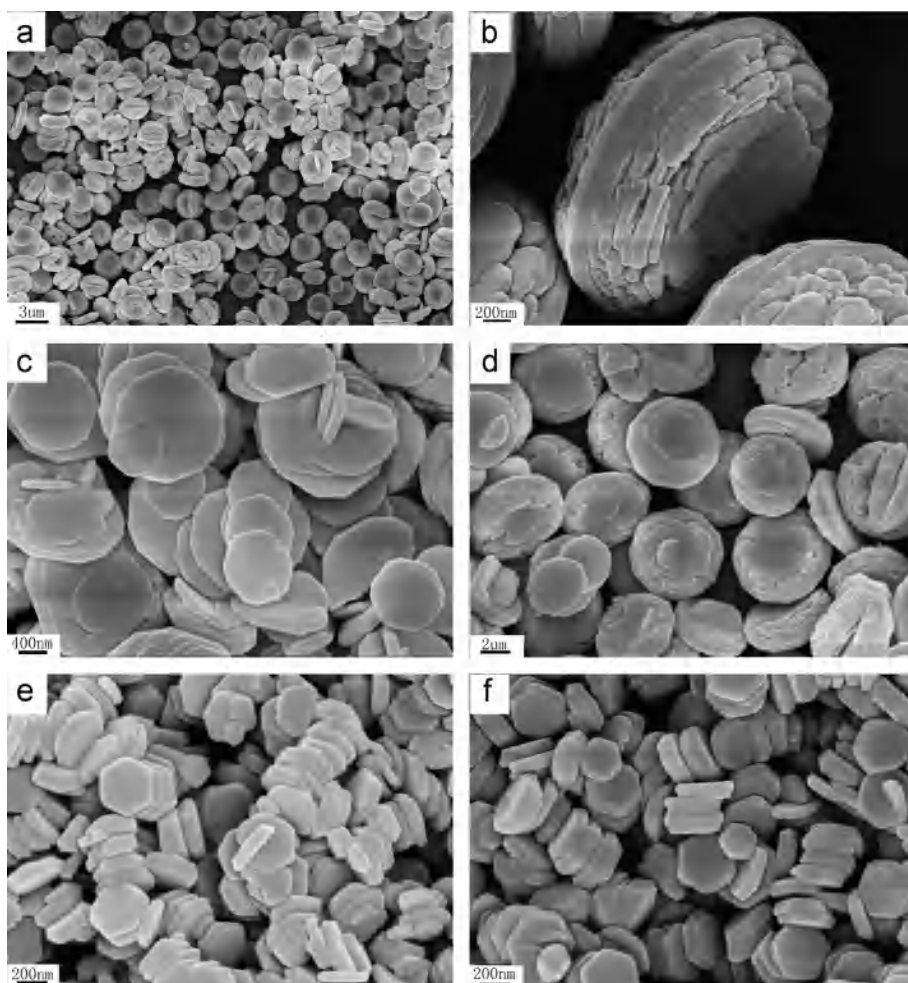


Fig. 2. SEM images of the as-prepared  $\text{CeF}_3$  when  $\text{N}(\text{C}_4\text{H}_9)_4\text{BF}_4$  was used in a period of: (a and b) 12 h; (c) 6 h; (d) 1 h and (e)  $\text{N}(\text{CH}_3)_4\text{BF}_4$  or (f)  $\text{NH}_4\text{BF}_4$  was used within 12 h.

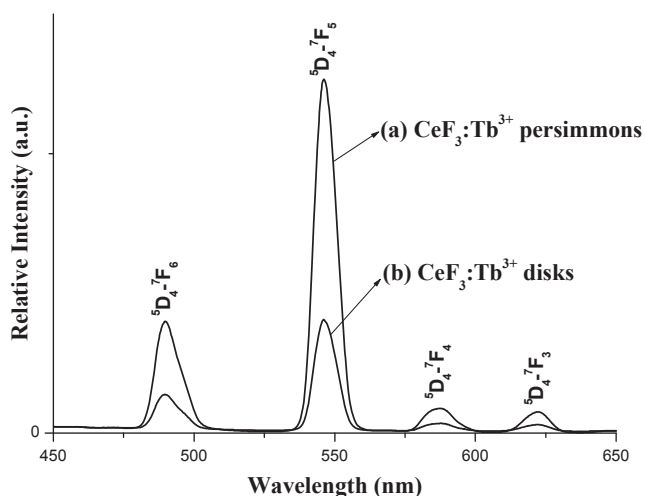


Fig. 3. Room temperature PL spectra of  $\text{CeF}_3:\text{Tb}^{3+}$  (a) hierarchical persimmon and (b) nanodisks.

Fig. 2a is the low magnified SEM image of the  $\text{CeF}_3$  obtained in a typical procedure, it can be seen that the as-prepared  $\text{CeF}_3$  are highly uniform and monodispersed persimmon-shaped structures with average diameters of 3  $\mu\text{m}$ . The magnified SEM images (Fig. 2b) from a single persimmon shows that the unique hierarchical structures are constructed by nanodisks and there is a concave dip in the center of each particle. As the assembled unit, the thickness of the nanodisk is thinner than 100 nm. Therefore, the fascinating hierarchical 3D architectures built from nanodisks were arranged in a particular way to layer-by-layer structures. These unique morphologies are similar to the reported hierarchical  $\text{LaF}_3$  [3]. Furthermore, in order to investigate the growth details of hierarchical persimmon-shaped  $\text{CeF}_3$  microstructures, time-dependent experiments were carried out. When the reaction time was 1 h, the SEM image (Fig. 2c) showed there were many polygonous disks with mean thickness of about 100 nm, and the diameters of the disks were different from each other. After reaction for 6 h, some of the nanodisks have assembled together into aggregates (Fig. 2d). The SEM image indicates that the layer-by-layer persimmon structures were constructed from many small primary nanodisks. With the prolonging of the reaction time, the hierarchical persimmon-shaped  $\text{CeF}_3$  microstructures undergo a self-assembly process in the morphological evolution. As much as we are concerned, little work has been conducted on hierarchical  $\text{CeF}_3$  assembled from nanodisks [12,16].

In order to investigate the effect of fluoride source, controlled experiments were performed. Other complex fluoride,  $\text{N}(\text{CH}_3)_4\text{BF}_4$  or  $\text{NH}_4\text{BF}_4$ , is used instead of  $\text{N}(\text{C}_4\text{H}_9)_4\text{BF}_4$  to synthesize  $\text{CeF}_3$  by an identical procedure. The SEM images of the product obtained from  $\text{N}(\text{CH}_3)_4\text{BF}_4$  or  $\text{NH}_4\text{BF}_4$  in a period of 12 h are shown in Fig. 2e and f. It can be seen that there are a large number of hexagonal nanoplates with diameter of 300–400 nm and thickness about 100 nm, and no hierarchical persimmons were formed. The above further affirmed the unique and crucial role of  $\text{N}(\text{C}_4\text{H}_9)_4\text{BF}_4$  in the formation of hierarchical persimmon-shaped  $\text{CeF}_3$ .

As we all know, the hydrolysis process of  $\text{BF}_4^-$  is very slow to produce  $\text{BO}_3^{3-}$  and  $\text{F}^-$  anions, and this step will keep the low concentration of  $\text{F}^-$  ions in the solution, and consequently leads to the slow crystallization process [3,19]. Firstly,  $\text{Ce}^{3+}$  reacted with  $\text{F}^-$  to form  $\text{CeF}_3$  primary nanoparticles. Then,  $\text{CeF}_3$  nanoparticles grow into 2D nanodisks because of their intrinsic layered crystal structure. In the following growth process, the organic molecule  $\text{N}(\text{C}_4\text{H}_9)_4\text{BF}_4$ , as capping reagent and structure director, can be selectively adsorbed on the surfaces of initially formed  $\text{CeF}_3$  to

change the surface properties and growth behavior. The obtained nanodisks began to assemble together to form persimmon-like microstructures. Therefore, the fluoride source has significant effect on the morphologies of the products.

The morphologies of the 5 mol%  $\text{Tb}^{3+}$  doped  $\text{CeF}_3$  samples have similar morphologies with the undoped  $\text{CeF}_3$ , this fact further proves that the morphologies of the samples are only affected by the fluoride sources. The luminescence properties of  $\text{CeF}_3$  doped with 5 mol% (molar ratio)  $\text{Tb}^{3+}$  ions with different morphologies were investigated. The room-temperature PL spectra of the as-synthesized  $\text{CeF}_3:\text{Tb}^{3+}$  were measured with an excitation source wavelength of 374 nm. As shown in Fig. 3, there were four major emission bands at 490 nm, 544 nm, 588 nm and 621 nm in each PL spectrum, and assigned to  $^5\text{D}_4 \rightarrow ^7\text{F}_6$ ,  $^5\text{D}_4 \rightarrow ^7\text{F}_5$ ,  $^5\text{D}_4 \rightarrow ^7\text{F}_4$ , and  $^5\text{D}_4 \rightarrow ^7\text{F}_3$ , respectively [3,19]. The strongest emission peak occurs at 544 nm. The emission spectrum is dominated by the  $^5\text{D}_4 \rightarrow ^7\text{F}_5$  transition of the  $\text{Tb}^{3+}$  ions [3]. It is worth noting that the intensity ratio of the peaks in the PL spectrum of the hierarchical persimmon-shaped  $\text{CeF}_3:\text{Tb}^{3+}$  is obviously enhanced compared with that of nanodisks. These results indicate that the luminescence properties of the nanostructured particles are largely affected by factors such as the morphology, the particle size, degree of crystallinity and the crystal structure.

#### 4. Conclusions

3D persimmon-shaped  $\text{CeF}_3$  hierarchical microstructures have been prepared via a simple hydrothermal route.  $\text{N}(\text{C}_4\text{H}_9)_4\text{BF}_4$  is used both as a fluoride source and structure directing agent to facilitate the morphological evolution process from nanodisks to nanodisk-assembled hierarchical architectures. The fluoride sources and reaction time play key roles in the formation of hierarchical  $\text{CeF}_3$  nano/microstructures.

#### Acknowledgments

This work was supported by the Natural Science Grant of China (No. 21173122, 21006054), Natural Science Foundation of Jiangsu Province of China (No. BK2010281) and Natural Training Programs of Innovation for Undergraduates (No. 201210304017).

#### References

- [1] Cölfen H, Mann S. *Angew Chem Int Ed* 2003;42:2350–65.
- [2] Cao XF, Zhang L, Chen XT, Xue ZL. *CrystEngComm* 2011;3:1939–45.
- [3] Wang M, Jiang GQ, Tang YF, Y.J. Shi. *CrystEngComm* 2013;15:1001–6.
- [4] Shimamura K, Villora EG, Nakakita S, Nikl M, Ichinose N. *J Cryst Growth* 2004;264:208–15.
- [5] Wang ZL, Quan ZW, Jia PY, Lin CK, Luo Y, Chen Y, et al. *Chem Mater* 2006;18:2030–7.
- [6] Qiu SQ, Dong JX, Chen GX. *Powder Technol* 2000;113:9–13.
- [7] Wang X, Zhuang J, Peng Q, Li YD. *Inorg Chem* 2006;45:6661–5.
- [8] Li CG, Li FF, Li T, Bai TY, Wang L, Shi Z, et al. *Dalton Trans* 2012;41:4890–6.
- [9] Liu Y, Zhao YB, Luo HJ, Wu ZS, Zhang ZJ. *J Nanopart Res* 2011;13:2041–7.
- [10] Li SA, Xie T, Peng Q, Li YD. *Chem Eur J* 2009;15:2512–7.
- [11] Qu X, Yang HK, Chung JW, Moon BK, Choi BC, Jeong JH, et al. *J Solid State Chem* 2011;184:246–51.
- [12] Liu Y, Zhao YB, Yu LG, Wu ZS. *J Alloys Compd* 2009;485:L1–4.
- [13] Dutta DP, Warrior S, Ghildayal R, Sharma G, Grover G, Tyagi AK. *J Nanosci Nanotechnol* 2009;9:4715–20.
- [14] Zhu L, Li Q, Liu XD, Li JY, Zhang YF, Meng J, et al. *J Phys Chem C* 2007;111:5898–903.
- [15] Ma L, Chen WX, Xu ZD. *Mater Lett* 2008;62:2596–9.
- [16] Ma L, Chen WX, Xu XY, Xu LM, Ning XM. *Mater Lett* 2010;64:1559–61.
- [17] Chai RT, Lian HZ, Li CX, Cheng ZY, Hou ZY, Huang SS, et al. *J Phys Chem C* 2009;113:8070–6.
- [18] Zhang H, Li HF, Li DQ, Meng SL. *J Colloid Interface Sci* 2006;302:509–15.
- [19] Wang M, Shi YJ, Jiang GQ, Tang YF. *Mater Lett* 2011;65:1945–8.